SHOCK CAPTURING SCHEMES FOR MULTIDIMENSIONAL FLOW

FINAL REPORT

by
Ijaz H. Parpia
Department of Aerospace Engineering
The University of Texas at Arlington
Arlington, TX 76019-0018

NASA Research Grant No. NAG 1 1207
January 18, 1991 – January 17, 1992

SHOCK CAPTURING SCHEMES FOR MULTIDIMENSIONAL FLOW

ABSTRACT

We report on progress made in the development of a 'genuinely multidimensional' finite-volume algorithm for problems in inviscid gasdynamics. The approach entails (a) the reconstruction of flowfield data using a planar wave pattern in which the strengths and orientations of the component waves are derived independently of the mesh geometry, and (b) the development of a flux formula which provides a numerical approximation to the flux at a finite-volume cell face during the passage of waves which are in general oblique to the face. We outline several algorithms, and include the most recent developments. The results of several numerical test cases are also included.

I. INTRODUCTION

The standard approach to modeling Euler flowfields in several space dimensions is to approximate the multidimensional solution operator by a sequence of one-dimensional operators applied along the mesh cooordinate directions. Several methods of this type are highly developed and have been applied successfully to a vast body of flow problems governed by the Euler and Navier-Stokes equations. The success of these methods is not, however, complete. Solution quality can be, in some instances, strongly mesh dependent. This is especially true in discontinuous regions whenever the dominant wave transition is oblique to the grid. This observation defines an obvious goal: to develop a grid-independent high-resolution flow solution algorithm.

The research undertaken during the grant period and described in this report is a preliminary effort in the development of such a scheme. The approach developed here is based on a local flowfield reconstruction through a pattern of grid-oblique waves. This approach reduces, in a natural way, the dependence of the solution on the grid geometry, and represents a significant step toward the realization of a grid-independent algorithm.

Research which predates the present work to improve wave resolution

in multidimensional flow includes the work of Davis,[1] Roe,[2] Hirsch *et al.*,[3] Powell and Van Leer,[4] and Levy *et al.*[5] These methods are outlined briefly below.

In the approach suggested by Davis, the passage of waves at an interface is modeled in a coordinate system which is locally rotated in such a way that the flow is nearly one-dimensional in the rotated frame. The input states for this rotationally-biased algorithm are determined by interpolation in the vicinity of the cell face. Davis assumes that the primary wave is a shock with normal aligned with the velocity jump across the interface. An upwind algorithm is used to compute the waves in the primary direction; terms which arise in the direction perpendicular to the primary waves are centrally differenced. Convergence is enhanced (at the expense of wave resolution) by smoothing the wave orientation information, and also freezing the wave angles at some stage during the calulations. This method produces solutions in which oblique shocks are resolved very well. Davis's procedure does not, however, explicitly account for a single wave of the stream type, because such a wave would be perpendicular to the specified shock direction.

Levy *et al.* have used a similar procedure to compute simple two-dimensional flows, and have explored a variety of choices for the local angle of rotation. In the continuation of this work, the use of upwinding algorithms in both the primary and perpendicular wave directions has been explored.

Roe's method entails the reconstruction of gradient data on a triangle. Because we use a similar reconstruction technique in one of the algorithms developed here, we defer the description of this method to Section II.

A conservative scheme based on the characteristic form of the Euler equations has been proposed by Hirsch *et al.* In this scheme, the underlying physics is modeled by the characteristic compatibility conditions written for the choice of wave normals which minimizes the coupling between waves. In other words, the governing system of equations is written in the form

$$\frac{\partial W}{\partial t} + \Lambda_x \frac{\partial W}{\partial x} + \Lambda_y \frac{\partial W}{\partial y} = R,$$

where W are the characteristic variables, such that R is minimized. Because the choice of normals determines the specific waves which are computed,

and because this choice depends on the gradients of the flow properties, this is a genuinely multidimensional approach. Powell and Van Leer have implemented a conservative algorithm based on this technique.

Other multidimensional algorithms, related to one or more of the methods described above, have been recently reported by Dadone and Grossman,[6] and by Kontinos and McRae.[7]

We begin with an outline of local flow reconstruction techniques investigated during the couse of this work. The flux formula is then developed in Section III, and the application of the most recently developed algorithm to several planar flow test cases is summarized in Section IV.

II. FLOWFIELD RECONSTRUCTION

In the finite-volume discretization of the flow problem, the physical region of interest is divided into a number of cells, and the distribution of flow properties within each cell is then specified according to some convenient approximation (for instance, that the flow properties are constant, or vary linearly in the cell). The wave system which governs the evolution of the flowfield is then constructed by matching the wave transitions to the local variations in the flow properties. The flowfield then evolves in a manner which is consistent with the passage of these waves, through the influence of the waves on the flux at the cell faces.

In this section we describe two methods by which the flowfield is reconstructed locally. The first is a Riemann method which is a generalization of the classical grid-aligned wave model.

Two-State Reconstruction

Given any two neighboring states in a flowfield, there are an infinite number of wave patterns by which the jump in state variables might be reconstructed. Clearly, additional rules are necessary to make the choice of waves unique. In the classical wave model, the waves are chosen to be oriented in a specified (grid-dependent) direction, and this choice, together

with a further restriction on the number of waves, leaves precisely enough free wave parameters (the wave strengths) to make the wave pattern unique for a given jump in states. The primary advantage of this technique lies in its simplicity. There is, as pointed out in the Introduction, a drawback in this reconstruction technique: High resolution of wave structures can be expected only if the true wavefront is aligned with the assumed (grid-aligned) wave direction. The failure of a grid-aligned wave model to properly describe oblique waves in multidimensional data has been recognized for some time (see, for example, Ref.2).

The investigation of two-state reconstruction techniques undertaken here, and reported in Refs. 8 and 9 evolved in parallel with the method of Rumsey *et al.*[10,11] As an aid to the description of the method, we introduce a remarkably useful picture of linearized state space,[†] due to Roe.[12] An arbitrary transition $(\delta u, \delta v, \delta p)$ between states l and r in planar flow is depicted in Figure 1 in a coordinate system in which the coordinate directions are chosen to be the pressure and the $x-$ and $y-$velocity components. The state l is placed at the origin, and the right state r is at the point $(\delta u, \delta v, \delta p)$. The envelope of possible transitions through acoustic waves with one endstate at l must lie on a cone with apex at l, because all such transitions satisfy the relation

$$|\delta p| = \rho a \sqrt{(\delta u)^2 + (\delta v)^2}. \tag{1}$$

All transitions across shear waves lie in horizontal planes. Note that density transitions are not representable on this diagram; thus an entropy wave cannot be depicted.

A superposition of k elementary wave transitions is used to reconstruct an arbitrary jump, that is

$$\delta V = \sum_{j=1}^{k} \delta V_j.$$

The problem is, of course, to determine the number, orientations, and strengths of the waves to be used. Assuming that the overriding requirement is single

[†]An efficient approach to shock capturing relies on the use of a local linearization technique which retains the important features of the nonlinear problem.[9,10] In what follows, we assume a local linearization, so that the state variables are replaced whenever appropriate by local averages. (For instance, ρ and a in (1) are average values).

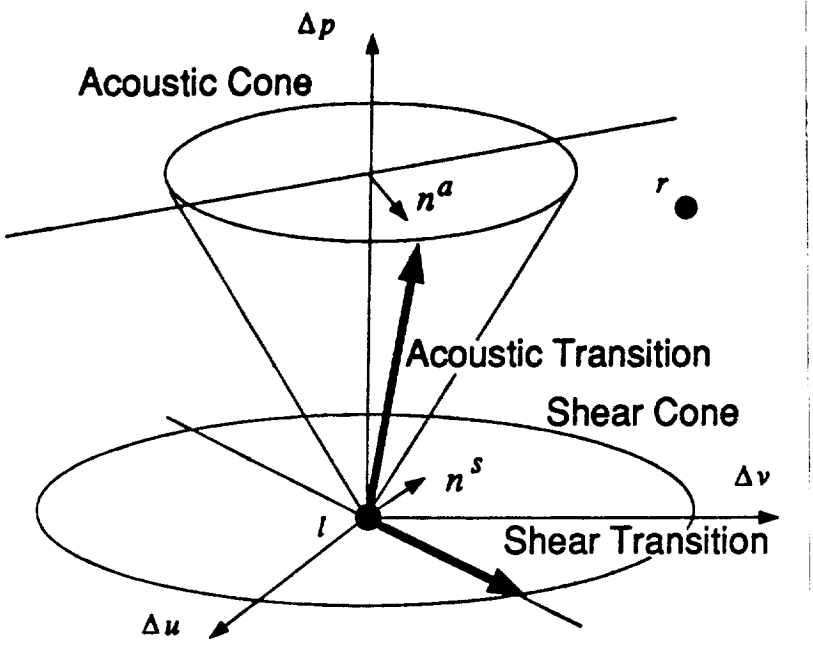

Figure 1: Elementary wave transitions in state space.

Rankine-Hugoniot wave recognition, any candidate wave model must return a single wave for this special case.

The type of wave pattern used in Refs. 8 – 11 to construct the state jump was guided by some measure of the closeness of the union of wave paths to the overall jump. If the number of waves is restricted to four (as in the grid-aligned case), the minimum path length choice leads to two acoustics and an entropy wave for r inside the acoustic cone; for r outside the cone, the waves are a forward- *or* a backward-facing acoustic, and a shear. The wave pattern specified here is shown in Figure 2. Note that the velocity jump across each acoustic and shear is parallel to the overall velocity jump (and the acoustic and shear waves are perpendicular to one another). A variety of other rules have been devised, and some of these are reported in Refs. 9 – 11.

Three-State Reconstruction

As we have seen above, two-state methods provide a local description of the flowfield based on the *jump* information between neighboring states.

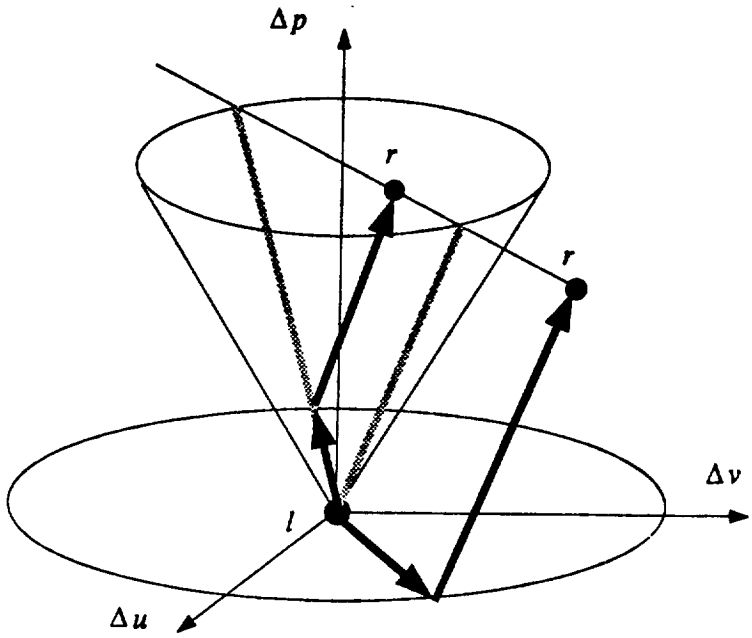

Figure 2: Minimum pathlength wave transitions.

Our experience with these methods has led to the conclusion that it is unreasonable to expect a realistic description of the local wave content of the flowfield based on this very restricted information (test results followed by further discussion of these methods appear in the remainder of this report).

A natural extension of the reconstruction technique entails the introduction of a third data point into the local description of the flow; this provides sufficient information to approximate flow *gradients.*[‡] This technique was first proposed by Roe.[2]

Three-point reconstruction fits naturally into the standard unstructured mesh discretization, in which the mesh consists of a set of nonoverlapping triangles. The data is assumed to be stored at the nodes; the data provides estimates of the flowfield gradients to which are matched the variations in flow properties described by the chosen wave pattern. There remains, of

[‡]The reconstruction of gradients makes it impossible to properly fit discontinuities into the data. This drawback is, however, of little importance, because the two-state reconstruction procedure is part of a solution algorithm which does not preserve perfectly-resolved discontinuities.

course, the difficulty of narrowing the choice of the wave pattern to a set which is unique for given data, and this issue is central to the reconstruction procedure.

In planar flow, there are eight derivatives, from which eight wave parameters can be found. One might therefore suppose that the natural choice in planar flow is a set of four waves (each of unknown strength and orientation), but a study of the planar-wave solutions of the Euler equations shows that the minimum number of waves (for arbitrary data) is in fact five, consisting of two acoustics, two shear waves, and an entropy wave. This is the choice we make in the algorithm described in Ref. 13. It is possible, of course, to specify a wave pattern with more than five waves; Roe and co-workers have proposed several six-wave models.[2,14] Finally, we observe that a reasonable choice of waves must also lead to simple algebra, otherwise the efficiency of the algorithm will suffer.

Because only eight wave parameters can be specified independently, additional rules are necessary to reduce the number of unknown wave parameters to precisely eight. The five-wave model proposed in Ref. 13 consists of a forward- and backward-facing acoustic wave pair with common normal, and a mutually perpendicular shear wave pair. This choice leads to the wave normals

$$\boldsymbol{n}^{\mathrm{ac}} = \frac{\nabla p}{|\nabla p|},$$

and

$$\boldsymbol{n}^{\mathrm{en}} = \frac{\nabla \rho - \rho/(\gamma p)\nabla p}{|\nabla \rho - \rho/(\gamma p)\nabla p|};$$

the first shear wave angle is

$$\theta_{\mathrm{shear}_1} = \frac{1}{2}\arctan\left\{\frac{(v_y - u_x) - \cos 2\theta_{\mathrm{ac}}\,(u_x + v_y)}{(v_x + u_y) + \sin 2\theta_{\mathrm{ac}}\,(u_x + v_y)}\right\}.$$

It is possible to derive expressions for the wave strengths directly from the data on the triangle, but a more robust algorithm results if the triangle data is now reconstructed by an edge-by-edge procedure, in which the wave patterns between pairs of states consist of waves with the above-specified orientations,

but with strengths found from the edge state jump. The expressions for the wave strengths α in terms of the state transition δV along an edge are

$$\alpha_{\mathrm{ac}_{1,2}} = \frac{1}{2}[\delta p \pm \rho a\, \delta \boldsymbol{u} \cdot \boldsymbol{n}^{\mathrm{ac}}],$$

$$\alpha_{\mathrm{en}} = \delta\rho - \frac{\rho}{\gamma p}\delta p,$$

and

$$\alpha_{\mathrm{sh}_1} = -\boldsymbol{n}^{\mathrm{sh}_2} \cdot \delta \boldsymbol{u}', \quad \alpha_{\mathrm{sh}_2} = \boldsymbol{n}^{\mathrm{sh}_1} \cdot \delta \boldsymbol{u}',$$

where

$$\delta \boldsymbol{u}' = \delta \boldsymbol{u} - \rho a\,(\alpha_{\mathrm{ac}_1} - \alpha_{\mathrm{ac}_2})\,\boldsymbol{n}^{\mathrm{ac}}$$

This edgewise procedure leads to an inconsistency, because the average states on the edges differ from the triangle-averaged state. This issue remains unresolved.

III. FLUX FORMULA

In this section, we give an account of the development of formulas to predict the numerical flux function. We begin with the flux function used in conjuction with the two-state reconstruction described earlier in this report.

Figure 3 depicts adjacent cells in the mesh; the flux is to be estimated at the common face. Suppose the wave pattern consists of mutually perpendicular waves, and we denote the orthogonal wave-aligned directions by the unit vectors $\boldsymbol{i}_n$ and $\boldsymbol{i}_t$. The upwind flux formula used in Refs. 8 – 11 can be interpreted as the flux estimate which arises from the assumption that the flux components in the wave aligned directions are

$$F^n = \frac{1}{2}\left[F_l^n + F_r^n - \sum |\delta F_w^n|\right],$$

where the sum is over waves with normal $\boldsymbol{i}_n$, and

$$F^t = \frac{1}{2}\left[F_l^t + F_r^t - \sum \left|\delta F_w^t\right|\right],$$

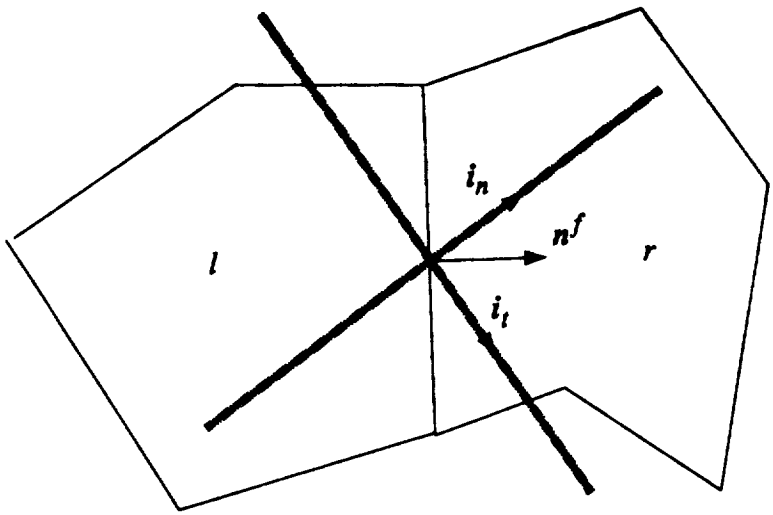

Figure 3: Figure for the derivation of the flux formula (2)

where the sum is over waves with normal $\boldsymbol{i}_t$. The face-normal flux is then

$$F^f = F^t \boldsymbol{i}_t \cdot \boldsymbol{n}^f + F^n \boldsymbol{i}_n \cdot \boldsymbol{n}^f = \frac{1}{2}\left[F_l^f + F_r^f - \sum \left|\delta F_w \boldsymbol{i}_w \cdot n^f\right|\right], \qquad (2)$$

where $\boldsymbol{n}^f$ is the cell face normal. This flux formula has also been applied in algorithms in which the two-state reconstruction includes waves of arbitrary relative orientation (for which the proper interpretation of the formula is not clear). As we shown in Section IV below, the use of this formula leads, in general, to highly nonmonotonic solutions.

A different flux formula, which has a clearer interpretation for waves of arbitrary orientation, has been developed for use in conjuction with the three-state reconstruction describe in Section III. The details of the development we outline below are presented in Ref. 13. The reader is also referred to Roe's original paper.[2]

We assume that the finite-volume cells are built from the triangle-centroid mesh dual shown in Figure 4. Then the cell faces are the edges of the polygonal cells, and we wish to estimate the flux on each face. Because the wave

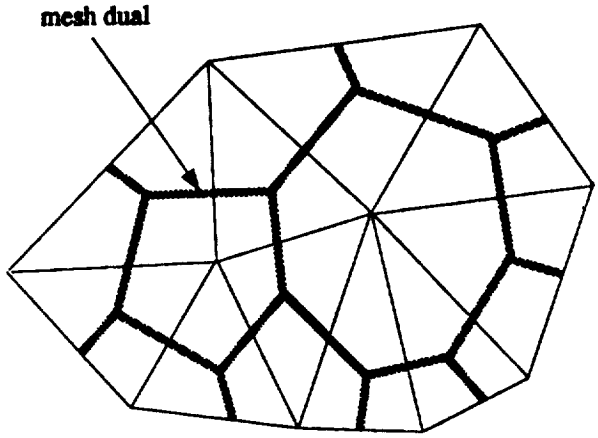

Figure 4: Finite-volume cells.

reconstruction is applied to the data on a triangle, we divide each cell face into the two pieces that are contained in adjacent triangles. The flux formula is then used to estimate the flux on partial-faces (which is equivalent to writing the flux on the full face as a weighted arithmetic average of the flux predicted on the two partial-faces).

Suppose each finite volume cell in Figure 4 is assembled from a set of triangles which are constructed by connecting the vertices of the polygonal cell to the center node. Such a triangle is shown in Figure 5. We now imagine a single plane wavefront passing through this triangle. Let the state ahead of the wave be denoted by the subscript r, and that behind the wave by l. The contour integral of the normal component of the flux tensor around the cell gives the simple result

$$\frac{\partial}{\partial t}\left(\bar{Q}A\right) = -s_w \delta F^w, \tag{3}$$

where A is the area of the triangle, s_w is the length of the wavefront inside the triangle, δF^w is the *normal* flux jump across the wave, and $\bar{Q}$ is the area-averaged value of the vector of conserved variables (mass, momentum,

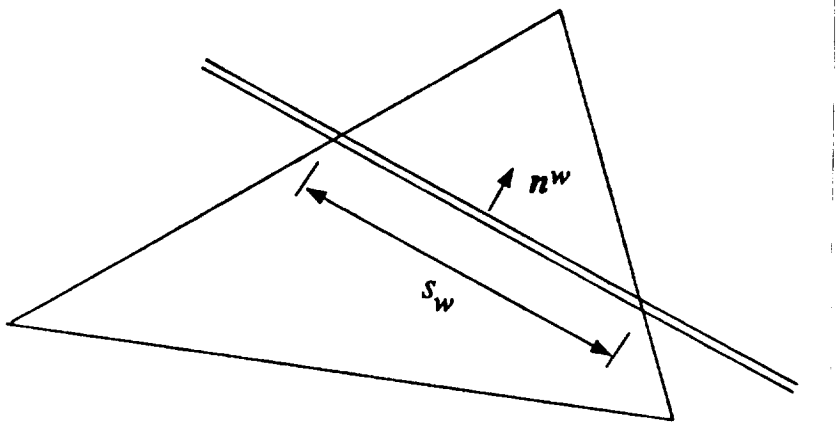

Figure 5: Wavefront passing through a triangular cell fragment

and energy per unit area). The result (3) is used below in the development of the numerical flux function.

Figure 6 depicts two triangular fragments of neighboring cells l and r. For algorithmic simplicity, we wish to account for the entire effect of the waves which arise between the states l and r through the numerical flux at the common face. This would obviate the need to explicitly calculate the effect of these waves on the remaining faces of the triangular segments. The manner in which this can be accomplished is to set the flux at the common face, normal to the face, to

$$F = F_l + \delta F^w \frac{s_w^l}{s_f}, \tag{4}$$

where s_w^l is an estimate of the length of the wave segment contained in the left triangle, and s_f is the face length. We note that it is equally valid to write

$$F = F_r - \delta F^w \frac{s_w^r}{s_f}, \tag{5}$$

and it is perhaps most reasonable to use the average of (4) and (5). Finally, for simplicity, we assume that ratio of the length of the wave segment to the cell face length is zero or unity, depending on the direction of motion of the

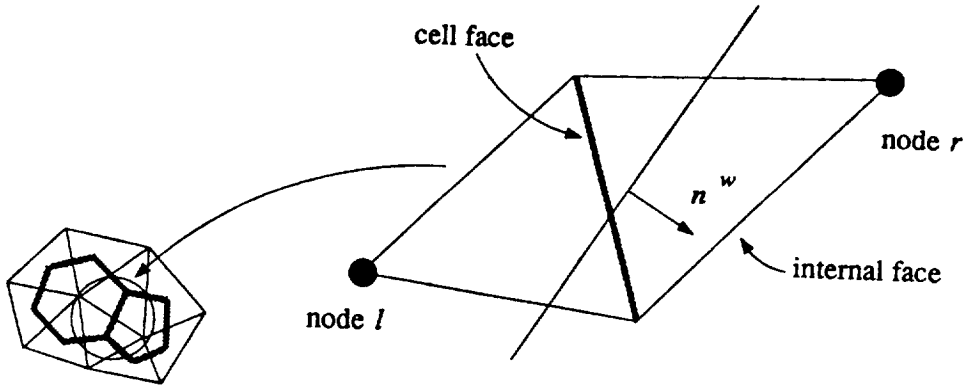

Figure 6: Neighboring triangular cell fragments

wave. This yields the flux formula

$$F = \frac{1}{2}\left[F_l + F_r - \sum_{k=1}^{5} \mathrm{sgn}(\lambda_k)\delta F_k^w\right], \tag{6}$$

where λ_k is the wave speed of the $k-$th wave, for a system of five waves.

It is interesting to note that the only difference in the flux formula used in Refs. 8 – 11, which was derived earlier in this section, and can be written in the form

$$F = \frac{1}{2}\left[F_l + F_r - \sum_{k=1}^{5} \mathrm{sgn}(\lambda_k)\delta F_k^w \left|\boldsymbol{n}_k^w \cdot \boldsymbol{n}^f\right|\right],$$

and equation (6) is the dot product term.

IV. TEST CASES

The methods described in this report have been tested on a array of simple two-dimensional flow problems. We show results for three channel flows, which cover the Mach number range from subsonic to high-supersonic.

Simple forward time integration with local time stepping is used in every case we show below.

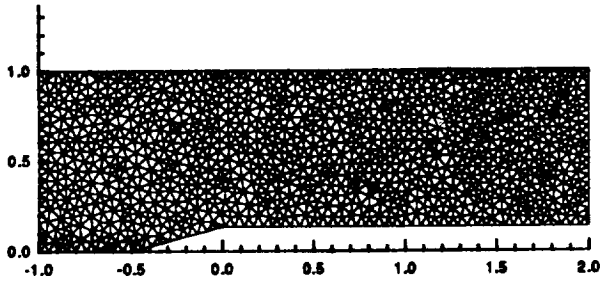

Figure 7: Channel geometry and grid.

The two-state reconstruction algorithm tested here on the supersonic channel flow differs slightly from earlier implementations: the method is applied here on an unstructured grid; the calculations presented in Refs. 8 and 11 we done on a structured grid. We also note that the finite-volume discretization is, for this algorithm, cell-centered.

Supersonic Channel Flow

This is the problem of Levy *et al.*[5] We present the geometry of the channel and a uniform 1074 node grid in Figure 7. The ramp angle on the lower wall is 15°. The Mach number contours shown in Figure 8 for an inflow Mach number of 2 show the solution obtained using the minimum pathlength two-state reconstruction and the flux formula (2). As this figure shows, although the wave resolution is good, the solution is clearly nonmonotonic. Furthermore, the maximum density residual diminshes only one order of magnitude over 1000 timesteps.

The same case was computed using the three-state reconstruction algorithm, together with the flux formula (6). Pressure and Mach number contours in Figures 9 and 10. These figure show that the variations in the flow properties are very nearly monotonic, and the resolution of the shockwaves is very high (2–3 triangles). The density residual history, shown in Figure 11, indicates better than two order-of-magnitude convergence in about 1000

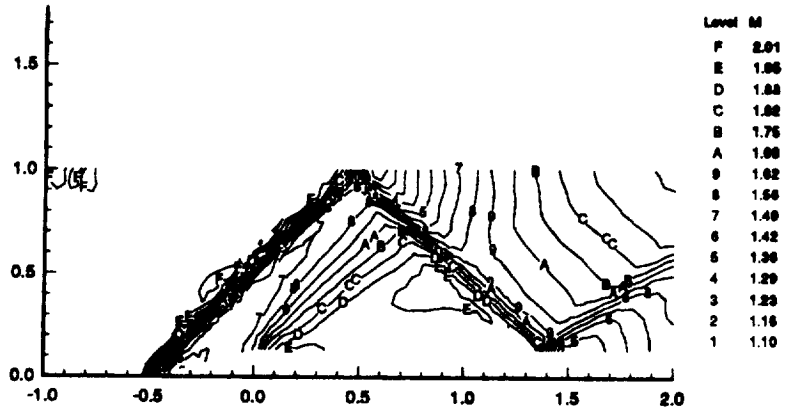

Figure 8: Mach number contours.

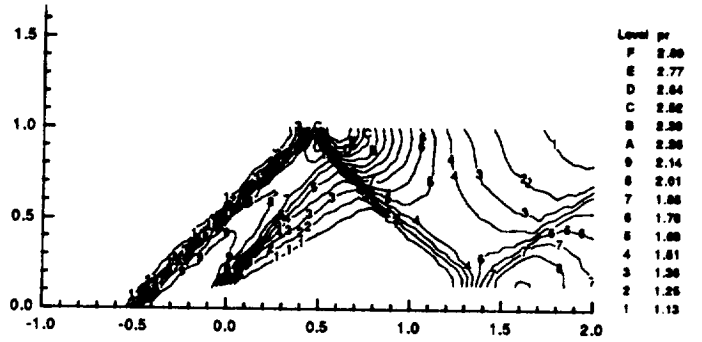

Figure 9: Pressure contours, method of Ref. 13.

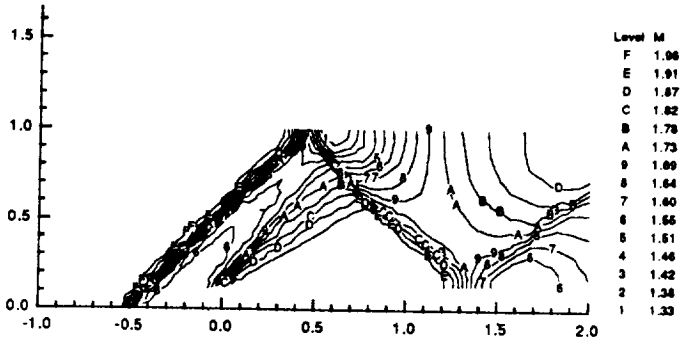

Figure 10: Mach number contours, method of Ref. 13.

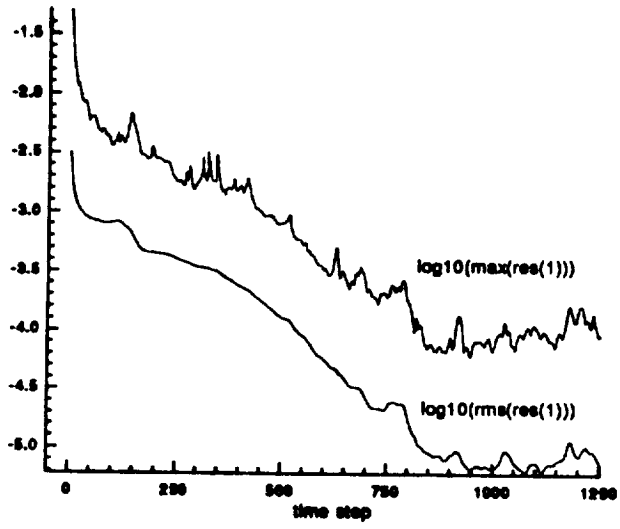

Figure 11: Density residual history for the supersonic channel flow problem

steps.

Double Ramp

The monotonicity of the algorithm of Ref. 13 is tested far more severely in this flowfield, which is a Mach 4 flow over a 20-35° double ramp. The uniform 1052 node grid we used is shown in Figure 12. Pressure and Mach number contours are plotted in Figures 13 and 14. The Mach number contours in Figure 14 clearly indicate the presence of the slip surface. These contour plots also show nearly-monotone variations in the flow properties. The density residual history in Figure 15 shows a two order-of-magnitude reduction in 500 timesteps.

Subsonic Channel Flow

The last test case we show here is a fully subsonic flow in the channel shown in Figure 16. The bump on the lower wall is a 10% circular arc, and

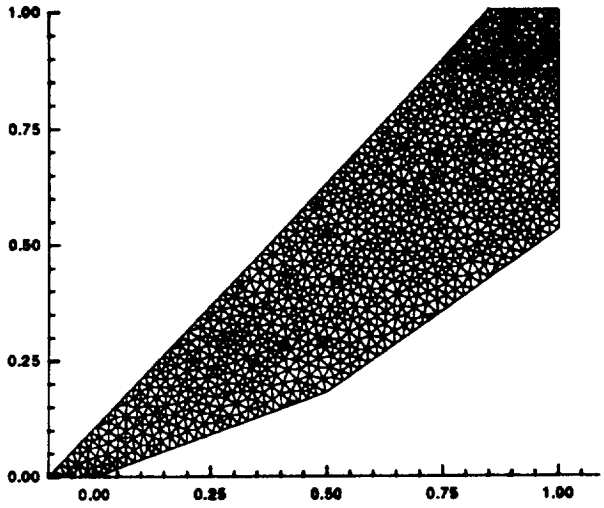

Figure 12: Ramp geometry and grid

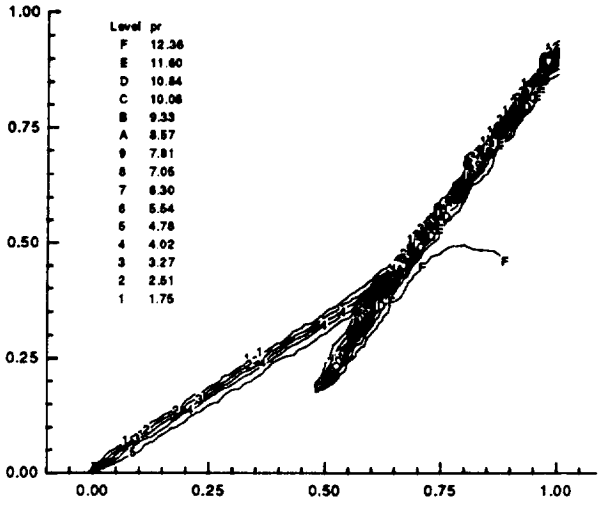

Figure 13: Pressure contours

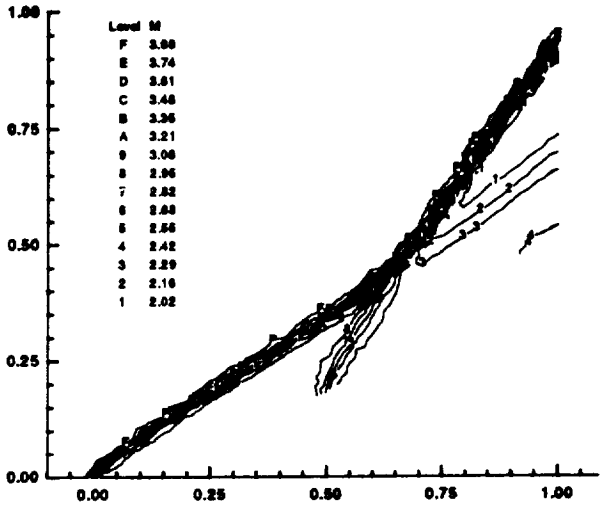

Figure 14: Mach number contours

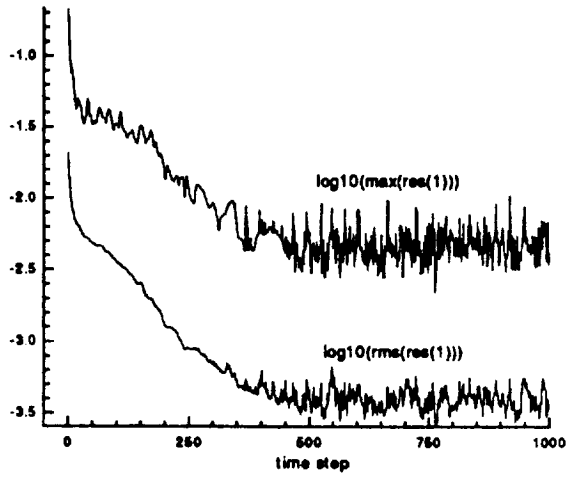

Figure 15: Density residual history for the double-ramp problem

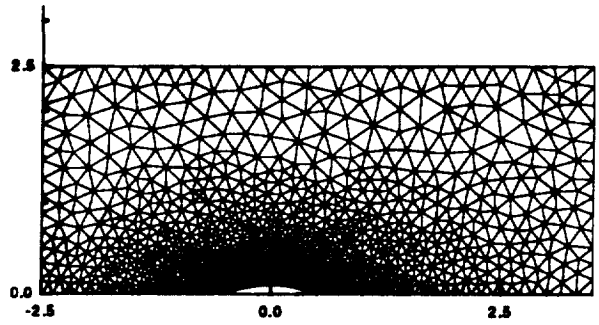

Figure 16: Channel geometry and grid

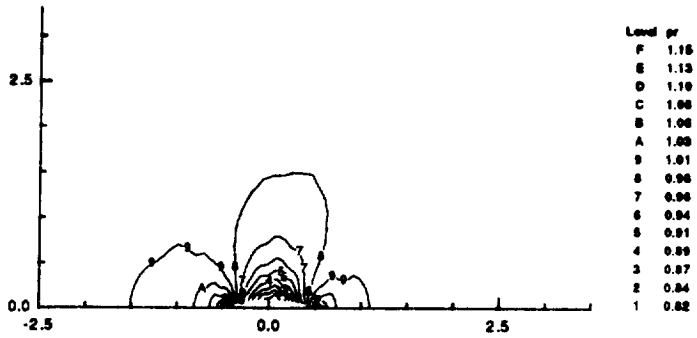

Figure 17: Pressure contours.

there are 29 nodes on the bump. The stretched grid contains a total of 1108 nodes. Pressure and Mach number contours for an inflow Mach number of 0.6 are shown in Figures 17 and 18. The more serious convergence problem alluded to earlier is apparent from the density residual history plot in Figure 19.

Discussion

It is immediately clear from these examples that the genuinely multidimensional methodology leads to very high wave resolution. Unfortunately,

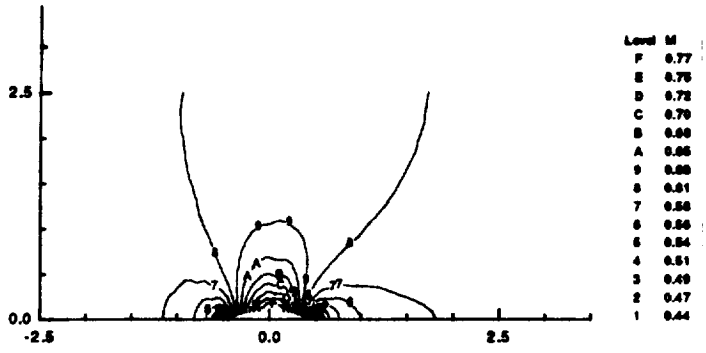

Figure 18: Mach number contours.

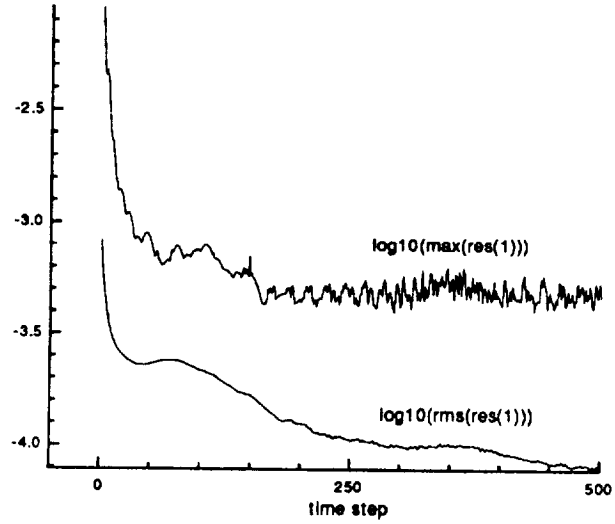

Figure 19: Density residual history for the subsonic channel flow problem

this comes at the cost of monotonicity and convergence. This is especially true of results using the two-state reconstruction method together with the flux formula (2). (A detailed study of the monotonicity behaviour of this family of methods is presented by Rumsey *et al.*[11])

There is a vast improvement in the quality of the solution when a three-state reconstruction is used with the new flux formula (6), but the solution still fails to be strictly monotonic, and convergence is not enhanced sufficiently. The lack of monotonicity and convergence is the most apparent in subsonic flow, perhaps because of the omnidirectional nature of propagation of acoustic signals. The wave model is designed to identify dominant waves in the data, and an added level of sophistication may be necessary to reconstruct data in which there are no strongly-preferred directions.

V. CONCLUDING REMARKS

Two major issues that have been raised repeatedly in the development of genuinely multidimensional schemes have yet to be resolved satisfactorily. The first of these is the nonmonotone behavior of solutions, and the second is the failure of the solution to converge to steady state. The developments described in this report address both of these issues, but it is clear that much remains to be done before methods of this type become viable replacements for classical grid-aligned schemes. On the other hand, genuinely multidimensional algorithms (both the finite-volume schemes discussed here, and the multidimensional fluctuation distribution algorithms proposed by Roe and co-workers) do show the potential to dramatically improve wave resolution, and at very little cost.

REFERENCES

1. S.F. Davis, "A rotationally biased upwind difference scheme for the Euler equations," *Journal of Computational Physics*, **56**, 1984.

2. P.L. Roe, "Discrete models for the numerical analysis of time-dependent multidimensional gasdynamics," *Journal of Computational Physics*, **63**, 1986.

3. C. Hirsch, C. Lacor, and H. Deconinck, "Convection algorithm based

on a diagonalization procedure for the multidimensional Euler equations," *AIAA Paper 87-1163*, Proceedings of the 8th Computational Fluid Dynamics Conference, Honolulu, HI, 1987.

4. K.G. Powell and B. van Leer, "A genuinely multidimensional upwind cell-vertex scheme for the Euler equations," *AIAA Paper 89-0095*, 27th Aerospace Sciences Meeting, Reno, NV, January 1989.

5. D.W. Levy, K.G. Powell, and B. van Leer,"An implementation of a grid-independent upwind scheme for the Euler equations," *AIAA Paper 89-1931-CP*, Proceedings of the 9th Computational Fluid Dynamics Conference, Buffalo, NY, 1989.

6. A. Dadone and B. Grossman, "A rotated upwind scheme for the Euler equations," *AIAA Paper 91-0635*, 29th Aerospace Sciences Meeting, Reno, NV, January 1991.

7. D. Kontinos and D. McRae, "An explicit, rotated upwind algorithm for solution of the Euler/Navier-Stokes equations," *AIAA Paper 91-1531-CP*, 10th Computational Fluid Dynamics Conference, Honolulu, HI, June 1991.

8. I.H. Parpia, and D.J. Michalek, "A shock capturing scheme for multidimensional flow," *AIAA Paper 90-3016-CP*, 8th Applied Aerodynamics Conference, Portland, OR, August 1990.

9. C.L Rumsey, B. van Leer, and P.L. Roe, "A grid-independent approximate Riemann solver with applications to the Euler and Navier-Stokes equations," *AIAA Paper 91-0239*, 29th Aerospace Sciences Meeting, Reno, NV 1991.

10. C.L. Rumsey, B. van Leer, and P.L. Roe, "Effect of a multidimensional flux function on the monotonicity of Euler and Navier-Stokes Computations," *AIAA Paper 91-1530-CP*, AIAA 10th Computational Fluid Dynamics Conference, Honolulu, HI, June 1991.

11. I. Parpia, "A planar oblique wave model for the Euler equations," *AIAA Paper 91-1545-CP*, AIAA 10th Computational Fluid Dynamics Conference, Honolulu, HI, June 1991.

12. B. van Leer, private communication, July 1990.

13. I.H. Parpia and D.J. Michalek, "A nearly-monotone genuinely multi-dimensional scheme for the Euler equations," *AIAA Paper 92-0325*, 30th Aerospace Sciences Meeting, Reno, NV, January 1992.

14. R. Struijs, H. Deconinck, P. de Palma, P. Roe, and K.G. Powell, "Progress on Multidimensional Upwind Euler Solvers for Unstructured Grids," *AIAA Paper 91-1550-CP*, AIAA 10th Computational Fluid Dynamics Conference, Honolulu, HI, June 1991.